Quantifying the Energetics of Cooperativity in a Ternary Protein Complex†

Peter S. Andersen,‡,§ Peter Schuck,|| Eric J. Sundberg,⊥ Carsten Geisler,‡ Klaus Karjalainen,# and Roy A. Mariuzza*,⊥

Institute of Medical Microbiology and Immunology, University of Copenhagen, Blegdamsvej 3C, DK-2200 Copenhagen N, Denmark, Division of Bioengineering and Physical Science, ORS, National Institutes of Health, 13 South Drive, Bethesda, Maryland 20892−5766, Center for Advanced Research in Biotechnology, W. M. Keck Laboratory for Structural Biology, University of Maryland Biotechnology Institute, 9600 Gudelsky Drive, Rockville, Maryland 20850, and Basel Institute for Immunology, Grenzacherstrasse 487, CH-4005, Basel, Switzerland

Received January 9, 2002; Revised Manuscript Received February 20, 2002

ABSTRACT: The formation of complexes involving more than two proteins is critical for many cellular processes, including signal transduction, transcriptional control, and cytoskeleton remodeling. Energetically, these interactions cannot always be described simply by the additive effects of the individual binary reactions that make up the overall complex. This is due, in large part, to cooperative interactions between separate protein domains. Thus, a full understanding of multiprotein complexes requires the quantitative analysis of cooperativity. We have used surface plasmon resonance techniques and mathematical modeling to describe the energetics of cooperativity in a trimolecular protein complex. As a model system for quantifying cooperativity, we studied the ternary complex formed by the simultaneous interaction of a superantigen with major histocompatibility complex and T cell receptor, for which a structural model is available. This system exhibits positive and negative cooperativity, as well as augmentation of the temperature dependence of binding kinetics upon the cooperative interaction of individual protein components in the complex. Our experimental and theoretical analysis may be applicable to other systems involving cooperativity.

Many of the most fundamental of cellular processes rely on the formation of complexes of multiple proteins, as they exceed the mechanistic limitations of simple binary binding reactions. The recent identification of vast networks of interacting proteins within the cell (*1*−*5*) has highlighted the interdependency of many of these processes and their reliance on such multiprotein complexes. Analysis of the associations of multiple proteins will likely become only more important in the post-genomic era as focus shifts from genomes to interactomes, the networks of protein−protein interactions encoded by whole genomes. While the rules that govern the interaction between two individual proteins in forming a bimolecular complex have yet to be fully elucidated (*6*−*10*), the association of more than two binding partners in a single multiprotein complex introduces further levels of complexity to the binding reaction that must also be addressed.

One hallmark of multiprotein complexes is cooperativity. As the affinity of proteins for their ligands is a fundamental property that determines the dynamic range within which they operate, binding capacity either gained or lost via cooperative interactions makes important contributions to the functionality of the resulting multiprotein complex (*11, 12*). To understand fully the role of cooperative binding in protein function, it is necessary to describe quantitatively each binary reaction that together comprise the multiprotein association and how each of these reactions is affected energetically by others in the overall complex. Studying the binding mechanisms of multiprotein complexes, however, is complicated by the intricacy of the reaction schemes, as well as the need for structural information and highly homogeneous sources of purified protein. While the rate at which atomic structures of multiprotein complexes are being described continues to increase, the energetic analysis of these higher order molecular interactions, in which cooperativity is likely to be a frequent attribute, has lagged well behind.

Presently, quantification of cooperative interactions involving proteins has been limited largely to oligomeric proteins binding nucleic acids (*13*−*17*) or cofactors (*18, 19*). These studies have provided valuable energetic detail to biological functions as diverse as the synergistic action of muliple transcription regulatory proteins at promoter and enhancer sites, mRNA turnover and translational efficiency, GTP hydrolysis, and ligand binding in the active pore of an enzyme. Measurements of cooperativity in these heterogeneous systems have generally required system-specific analysis techniques, such as quantitative DNase I footprinting titration or stopped-flow flourescence anisotropy. However, these techniques are not necessarily applicable to the study of cooperative systems involving only protein species, and

† This work was supported by grants from the Danish Medical Research Council, the Danish Cancer Society, and the National Institutes of Health. E.J.S. is supported by a fellowship from the Arthritis Foundation. P.S.A. was supported by fellowships from the Danish Natural Science Research Council and the Danish Medical Research Council.

* To whom correspondence should be addressed. Telephone: (301) 738-6243. Fax: (301) 738-6255. E-mail: mariuzza@carb.nist.gov.

‡ University of Copenhagen.

§ Present address: Symphogen A/S, Elektrovej, Building 375, DK-2800 Lyngby, Denmark.

|| National Institutes of Health.

⊥ University of Maryland Biotechnology Institute.

Basel Institute for Immunology.

10.1021/bi0200209 CCC: $22.00
Published on Web 03/29/2002

thus techniques that are not system-dependent will often be required for their analysis.

Here, we present a quantitative analysis of cooperativity in a model ternary protein complex. In our model system, we have quantified both negative and positive cooperative interactions in a complex that exhibits an overall increase in affinity due to cooperativity. We also show that the temperature dependence of binding kinetics increases significantly on account of the cooperative interactions of the three protein binding partners. Our methods of analysis rely on surface plasmon resonance (SPR)[1] techniques and mathematical modeling using standard laws of mass action and of mass balance to quantify cooperativity. While not absolutely required, an accurate structural model aided significantly in the interpretation of the energetic data. As our experimental and theoretical approach to measuring cooperativity is not specific to our model system, it may prove appropriate for quantifying cooperativity in other higher order protein complexes. The growing number of multiprotein complexes whose three-dimensional structures have been determined provides a rapidly expanding array of potential targets for further energetic analysis of cooperative binding (*20*−*22*), perhaps using the approach described here.

EXPERIMENTAL PROCEDURES

Protein Expression and Purification. Soluble 14.3.d T cell receptor (TCR) $\alpha\beta$ heterodimer was produced in SL-3 *Drosophila* cells as described previously (*23*). Soluble TCR β chain was produced in transfected myeloma cells (*24*). Recombinant protein was purified from culture supernatants using affinity chromatography followed by ion exchange chromatography. The major histocompatibility complex (MHC) class II molecule HLA−DR1 (DR1) was produced by in vitro refolding from *E. coli* inclusion bodies according to published methods (*25*). Staphylococcal enterotoxin C3 (SEC3) and the SEC3 phage display variant 3B2 (3B2) were expressed as soluble proteins in *E. coli* and isolated from the periplasmic fraction as described previously (*26*).

Binding Analysis. SPR studies were performed using BIAcore X and BIAcore 2000 instruments. General experimental conditions were as described previously (*26*, *27*). Proteins were immobilized onto the sensor surface using standard amine coupling chemistry, and experiments were performed using HBS running buffer. To quantify the cooperative effect, two comprehensive data sets were generated independently, each consisting of a titration series for the pairwise and ternary binding isotherms. In each data set, two flow cell surfaces were coupled with relatively low densities of TCR $\alpha\beta$ heterodimers, and a third flow cell surface was coupled with TCR β chains. Surface densities were chosen that corresponded to a maximum binding of 3B2 of ~500 RU. A fourth flow cell served as negative control to allow subtraction of the bulk refractive index. Dilutions of 3B2 and DR1, ranging from 0.04 to 200 μM and from 0.03 to 30 μM, respectively, were combined totaling 55 and 34 different mixtures. Each mixture was passed serially over the four sensor surfaces at a flow rate of 10 μL/min and allowed to bind until equilibrium was reached, followed by observation of the dissociation phase. The response of the blank surface was subtracted from all data prior to the analysis. The amount of ternary complex formed on TCR $\alpha\beta$ heterodimer coupled surfaces was estimated from the dissociation phases by extrapolation to the start of the dissociation phase using the known half-life of the ternary complex of 22 s. On the TCR β chain surface, total binding at equilibrium was recorded for each mixture of 3B2 and DR1 [with TCR β chain, the slow dissociation phase of the ternary complex is absent (*26*)]. Bimolecular interactions were studied under conditions similar to those used for the ternary complex. The binding of 3B2 to TCR $\alpha\beta$ heterodimer was evaluated by injecting increasing concentrations of 3B2 over each of the four flow cells described above (Figure 3B, lower inset). The K_d of the DR1−3B2 interaction was determined in two ways. First, 3B2 was immobilized, and serial dilutions of DR1 ranging from 0.4 to 24 μM were allowed to bind. Fitting of isotherms yielded the K_d to immobilized 3B2 (Figure 3B, upper inset, in blue). Second, the binding between 3B2 and DR1 in solution was determined by mixing 2 μM DR1 with serial dilutions of 3B2 (from 0.04 to 200 μM) and passing these mixtures over a 3B2-coupled surface. K_d in solution was then determined by fitting equilibrium binding to a competition model (Figure 4B, upper inset, in green). Determination of their solution binding constant was important with regard to the precise prediction of ternary complex formation. The final data sets consisted of 199 and 135 unique data points, respectively, and their mathematical modeling is described below. A separate, less comprehensive, data set of 77 data points made on a single TCR $\alpha\beta$ heterodimer coupled surface (including background subtraction) yielded fits of similar quality that resulted in values virtually identical to those obtained using the more comprehensive data sets. Average results of the three fitting procedures are presented in Table 1. Each complete set of isotherms was fitted globally, which included the titration of immobilized 3B2 with soluble DR1 [with equilibrium association constant $K_{D,S(surf)}$], the solution interaction between 3B2 and DR1 ($K_{D,S}$) in the competition experiment, the titrations of immobilized TCR $\alpha\beta$ heterodimer and TCR β chain with soluble 3B2 ($K_{S,T}$), and the experiments with different equilibrium mixtures of soluble 3B2 and soluble DR1 interacting with immobilized TCR (two data sets for TCR $\alpha\beta$ heterodimer or one data set for TCR β chain) which revealed the binding constant $K_{DS,T}$ of the DR1−3B2 complex to TCR $\alpha\beta$ heterodimer or TCR β chain, respectively. As described above, the latter data included either the plateau isotherms or the estimated ternary complex, respectively. Binding experiments at different temperatures were conducted essentially as described above except that the flow rate was adjusted to 20 μL/min. When possible (DR1 molecules did not tolerate the immobilization procedure), these experiments were repeated in the reverse orientation to confirm that the observed temperature dependencies were independent of assay orientation (data not shown).

RESULTS AND DISCUSSION

A Model System for Quantifying Cooperativity in Multiprotein Complexes. As a model system for quantifying

[1] Abbreviations: 3B2, SEC3 phage display variant 3B2; DR1, MHC class II human leukocyte antigen DR1; MHC, major histocompatibility complex; RU, resonance unit; SEC3, staphylococcal enterotoxin C3; SPR, surface plasmon resonance; TCR, T cell receptor.

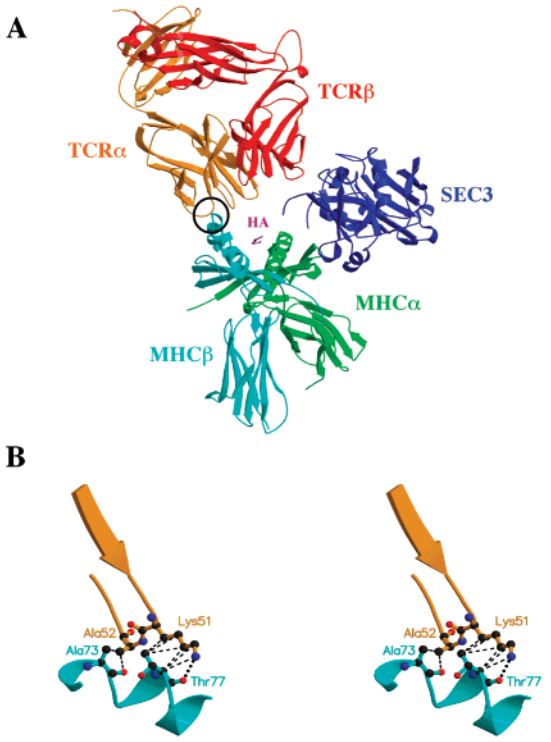

FIGURE 1: Structural model of the TCR−SEC3−DR1 complex. (A) Model of the MHC−SEC3−TCR αβ heterodimer complex produced by superimposing the HLA−DR1(HA 306−318)−SEC3 complex (E.J.S., P.S.A., and R.A.M., unpublished results), the SEC3−14.3.d TCR β chain complex (*30*), and the 2C TCR αβ heterodimer complex (*29*). Overlapping SEC3 and TCRβ molecules have been removed for clarity. Colors are as follows: SEC3, blue; MHC α subunit, green; MHC β subunit, cyan; HA(306−318) antigenic peptide, magenta; TCR α chain, orange; TCR β chain, red. (B) Molecular modeling of the DR1 β subunit−TCR α chain interface. Interactions between residues Lys51 and Ala52 from the CDR2 loop of the Vα and residues Ala73 and Thr77 from the DR1β subunit. van der Waals interactions are indicated by dashed lines, and a potential hydrogen bond between the N^{ζ} atom of Lys51 and the main chain carbonyl O of Thr77 is indicated by a dotted line. Intermolecular contacts were defined by atomic pair distances (in Å) less than or equal to the following: C−C, 4.1; C−N, 3.8; C−O, 3.7; N−N, 3.4; N−O, 3.4; O−O, 3.3. Colors are as follows: MHC β subunit, cyan; TCR α chain, orange; carbon atoms, black; nitrogen atoms, blue; oxygen atoms, red.

cooperative interactions, we utilized a triple protein complex consisting of the bacterial superantigen SEC3 in association with soluble forms of the human MHC class II molecule HLA−DR1, and a murine TCR αβ heterodimer (Vβ8.2/Vα4.2). Superantigens activate T cells by interacting simultaneously with the Vβ domain of the TCR αβ heterodimer and the α subunit of the MHC molecule (*24*). Although no experimentally determined structure of the MHC−SEC3−TCR complex exists, crystal structures of SEC3−DR1 (E.J.S., P.S.A., and R.A.M., unpublished data), the murine 2C TCR αβ heterodimer (*29*), and SEC3−TCR β chain (*30*) complexes make it possible to construct a structural model for the ternary complex by superimposing the common elements of these individual binary complexes. This model predicts that SEC3 acts as a wedge prohibiting the MHC-bound antigenic peptide from contacting the hypervariable loops of the TCR (Figure 1A). The ternary complex is stabilized through three distinct protein−protein interfaces: SEC3−MHC α subunit; SEC3−TCR Vβ domain; and TCR Vα domain−MHC β subunit. As the only interface of the three that has not been defined crystallographically, we have visualized the MHC β subunit−TCR α chain interaction by substituting the mVα4.2 CDR2 loop residues into the ternary complex model of Figure 1A. The resulting model was subjected to rigid-body refinement and conjugate gradient minimization without X-ray terms using CNS (*31*), indicating a relatively small interface of 396 $Å^2$ (using a probe radius of 1.4 Å). The predicted interface consists of eight van der Waals interactions between main chain and side chain atoms of residues Ala73 and Thr77 of the MHC β subunit and residues Lys51 and Ala52 of the Vα4.2 CDR2 loop, as well as one hydrogen bond between the N^{ζ} atom of Lys51 and the main chain O of Thr77 (Figure 1B).

Biochemical and crystallographic studies have demonstrated that isolated TCR β chain can interact functionally with SEC3 (*30*, *32*, *33*). The contribution of DR1 β subunit−TCR α chain contacts can therefore be addressed directly by comparing DR1−SEC3−TCR complex formation in the absence and presence of the TCR α chain (*26*). By making mathematical models based on the laws of mass action and of mass balance, it becomes possible to obtain estimates of the cooperative effect by globally fitting binding isotherms of varying concentrations of DR1 and SEC3 interacting with TCR fragments immobilized on biosensor surfaces. The low affinity of the wild-type SEC3−DR1 interaction, however, precludes the collection of sufficiently resolved binding data to quantify the cooperative effect (data not shown). Previously, we had created a SEC3 variant, 3B2, with 50-fold increased affinity for DR1 by phage display through randomization of a portion of the SEC3 surface (*26*). The increased affinity of 3B2 for DR1 enhanced significantly the quality of the ternary complex binding data, and this variant was therefore used as a reagent in all subsequent experiments. The mutated residues of 3B2 are entirely buried against the surface of DR1 (E.J.S., P.S.A., and R.A.M., unpublished data) and therefore cannot contact the TCR component of the ternary complex. Thus, the energetic contributions of the contacts between the DR1 and TCR molecules in the ternary complex are presumed to be equal whether the cross-linking reaction utilizes SEC3 or 3B2.

Initial experiments confirmed that binding of 3B2 to immobilized TCR αβ heterodimer increased in the presence of increasing concentrations of DR1 (Figure 2A). When examining binding to the TCR β chain alone, however, the reverse effect was observed: increasing amounts of DR1 caused a drop in the TCR binding of 3B2 (Figure 2B). This clearly shows a differential effect of 3B2−DR1 complex binding to TCR αβ heterodimer and TCR β chain molecules and suggests that both positive and negative cooperative binding is involved in the formation of the ternary complex. Most bacterial superantigens possess a highly flexible, disulfide-bridged loop located between their TCR and MHC combining sites. Indeed, uninterpretable electron density exists for this loop region in both the SEC3−DR1 and 3B2−DR1 (E.J.S., P.S.A., and R.A.M., unpublished data) and SEC3−TCR β chain (*30*) crystal structures. Binding of SEC3 or 3B2 at one site could potentially displace the loop in the direction of the opposing site and thereby reduce its accessibility. Such a mechanism could explain the negative cooperativity between the two 3B2 combining sites. In fact, we have isolated other SEC3 variants by phage display with

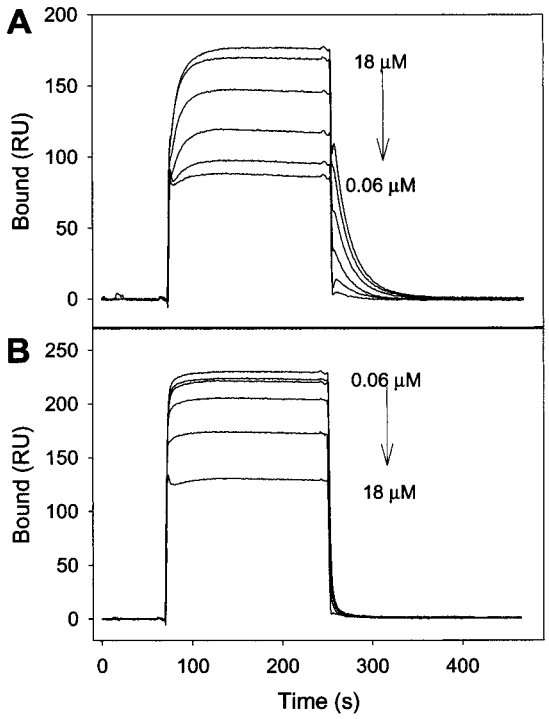

FIGURE 2: Positive and negative cooperative effects are involved in ternary complex formation. (A) Overlay sensorgrams of soluble 3B2 (3.8 μM) binding to immobilized TCR $\alpha\beta$ heterodimer in the presence of increasing concentrations of DR1 (0.06, 0.18, 0.60, 1.8, 6.0, and 18μM as indicated). (B) 3B2 and DR1 binding to immobilized TCR β chain. Concentrations of 3B2 and DR1 are as in (A).

mutations in the disulfide loop that exhibit increased TCR affinity in which the loop, when TCR bound, inhibits MHC binding (*34*).

The mixed cooperative nature of this ternary complex complicates determination of the positive cooperativity component because of the possibility that the TCR α chain may be partially lost during the immobilization procedure, which would render the TCR $\alpha\beta$ heterodimer-coupled surface a mixture of TCR $\alpha\beta$ heterodimer and TCR β chain molecules. To avoid the problem of a heterogeneous surface in our analysis, estimates of positive cooperative binding on TCR $\alpha\beta$ heterodimer-coupled surfaces were based only on the amount of full ternary complex, easily determined due to the significant difference in dissociation kinetics (for example, compare dissociation phases in Figure 2A,B). In contrast, negative cooperativity was evaluated as total binding on TCR β chain coated surfaces, assumed to be homogeneous.

Mathematical Modeling of Binary and Tertiary Binding Isotherms. Langmuir isotherms were used to model the binding of soluble DR1 at a concentration, [D], with immobilized 3B2, $[S_{surf}]$, forming a surface complex, $[DS_{surf}]$, as well as the binding of soluble 3B2, [S], with immobilized TCR, [T], to form complex $[ST_{surf}]$ at the surface:

$$[DS_{surf}] = [S_{surf}]_{tot}\frac{1}{1 + (K_{DS}^{surf}[D])^{-1}} \quad (1)$$

$$[ST_{surf}] = [T]_{tot}\frac{1}{1 + (K_{ST}^{surf}[S])^{-1}} \quad (2)$$

For the analysis of the solution competition experiments with soluble 3B2 [S] and a fixed concentration of soluble DR1 $[D]_0$ (Figure 3B, upper inset), mass conservation and mass balance leads to the well-known expression for the concentration of free DR1, $[D]_{free}$:

$$[D]_{free} = [D]_0 - 0.5\left\{[S] + [D]_0 + \frac{1}{K_{DS}^{sol}} - \left(\left([S] + [D]_0 + \frac{1}{K_{DS}^{sol}}\right)^2 - 4[S][D]_0\right)^{0.5}\right\} \quad (3)$$

which is subject to surface binding according to eq 1. For the interactions with immobilized TCR, mass balance was imposed for the total number of surface sites ($[T]_{tot}$), the free sites ($[T]_{free}$), and the sites liganded by 3B2 ($[ST_{surf}]$) and by a 3B2−DR1 complex ($[DST_{surf}]$): $[T]_{tot} = [T]_{free} + [ST_{surf}] + [DST_{surf}]$ (no interaction of free DR1 with TCR occurs, as this murine TCR does not recognize specifically the human HLA−DR1 molecule). Similarly, when using mixtures of 3B2 and DR1 to study ternary complex formation, mass balance should be obeyed in the solution phase for the total concentration of 3B2, $[S] = [S]_{free} + [DS]$, and for the total DR1 concentration, $[D] = [D]_{free} + [DS]$, with [DS] denoting the complex of 3B2 and DR1 in solution according to the mass action law: $K_{DS}^{sol} = [DS]/[S]_{free}[D]_{free}$ (the surface concentrations can be neglected relative to the solution concentrations because of the small absolute number of surface sites, and because of the constant flow of the equilibrium mixture of 3B2 and DR1). Finally, we used the mass action law for surface binding of 3B2: $K_{ST}^{surf} = [ST]/[S]_{free}[T]_{free}$, and, separately, for the surface binding of preformed 3B2−DR1 complex: $K_{DST}^{surf} = [DST]/[DS][T]_{free}$. These equations were solved simultaneously, leading to an expression for the concentration of free 3B2 in solution analogous to eq 3, for the surface concentration of 3B2 bound to TCR:

$$[ST] = [T]_{tot}\frac{K_{ST}^{surf}[S]_{free}}{1 + (K_{ST}^{surf} - K_{DST}^{surf})[S]_{free} + K_{DST}^{surf}[S]} \quad (4)$$

and for the surface concentration of ternary complex:

$$[DST] = [T]_{tot}\frac{K_{DST}^{surf}([S] - [S]_{free})}{1 + (K_{ST}^{surf} - K_{DST}^{surf})[S]_{free} + K_{DST}^{surf}[S]} \quad (5)$$

These isotherms can be used to model the binary and ternary complex at the TCR surface as a function of total 3B2 and DR1. The surface concentrations were transformed into SPR signal contributions by taking into account the molar mass of the respective complexes, and eqs 1−5 were fit globally to the respective experimental data sets, using binding constants as global parameters.

Quantifying the Free Energy of Cooperativity. To make a comprehensive data set defining the two-dimensional binding isotherm, 3B2 and DR1 were diluted serially and mixed at different molar ratios. Each mixture was passed over TCR $\alpha\beta$ heterodimer and TCR β chain coupled surfaces and allowed to bind until equilibrium was reached. Binary interactions were performed in parallel. 3B2 dilutions were passed over the same TCR-coupled surfaces in the absence

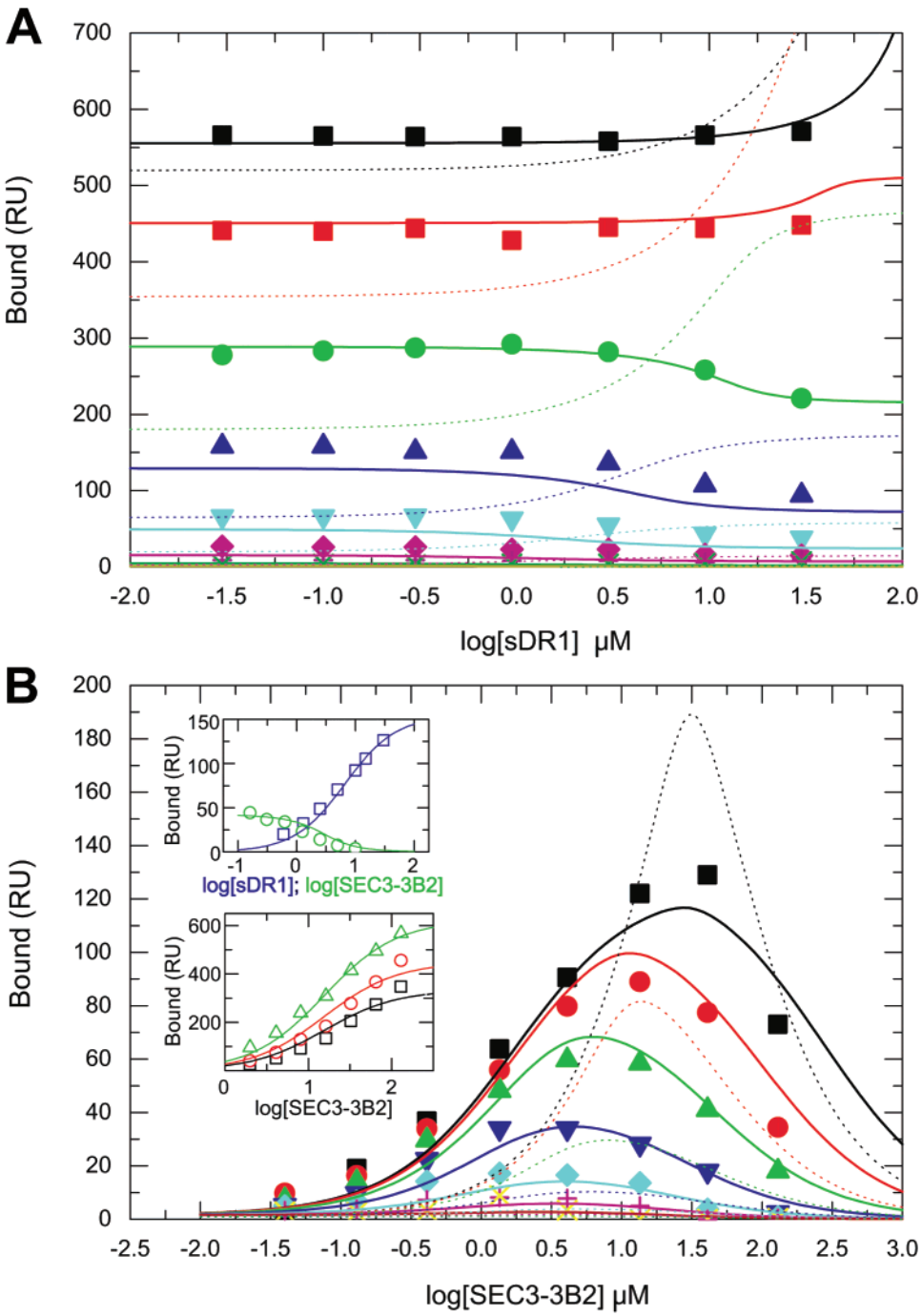

FIGURE 3: Fitting of ternary complex binding results. Representative plots of the global fitting procedure. Solid lines are calculated best-fit isotherms for a model including cooperative binding. For comparison, dotted lines represent the best-fit isotherms calculated in the absence of cooperative binding. (A) Binding to immobilized TCR β chain of varying concentrations of DR1 mixed with 3B2 at 130 μM (black squares), 41 μM (red squares), 14 μM (green circles), 4.1 μM (blue trangles), 1.4 μM (light blue trangles), 0.4 μM (purple diamonds), or 0.14 μM (yellow crosses). In this representation, in the absence of any DR1 binding to 3B2, horizontal lines would be expected that would define the binary 3B2−TCR isotherm. Deviation from the horizontal lines reflects both the increased signal due to the increased mass of a DR1−3B2 complex, as well as cooperativity effects of bound DR1 on the 3B2−TCR β chain interaction. (B) Amount of ternary complex formed on immobilized TCR $\alpha\beta$ heterodimer using varying concentrations of 3B2 mixed with DR1 at 30 μM (black squares), 9.5 μM (red circles), 3.0 μM (green triangles), 1.0 μM (blue trangles), 0.3 μM (light blue diamonds), 0.1 μM (purple crosses), or 0.03 μM (yellow crosses). These isotherms reflect the ratio of free 3B2 to 3B2−DR1 complex in solution offered to the immobilized TCR $\alpha\beta$ heterodimer. At a fixed concentration of DR1, increasing 3B2 leads to higher 3B2−DR1 complex concentrations available for ternary surface complex formation. At 3B2 concentrations higher than an optimal value, most surface sites will be occupied with unliganded 3B2. Upper inset in (B) shows dilutions of DR1 binding to immobilized 3B2 (blue squares) and dilutions of 3B2 competing out binding of DR1 to immobilized 3B2 (green circles). Lower inset in (B) shows binding of 3B2 to two TCR $\alpha\beta$ heterodimer coupled surfaces (red circles and black squares) and one TCRβ surface (green triangles). The data shown in the insets contain the information on the binary 3B2−TCR and 3B2−DR1 interactions.

of DR1 molecules. The affinity of 3B2 for DR1 was evaluated by solution competition in order to obtain an estimate of the true DR1−3B2 affinity in solution, since this was the condition used to study formation of the ternary

Table 1: Summary of Binding Constants

	units	SEC3	3B2
Previous Estimates			
$K_{d(SEC3/TCR)}$	μM	22[a]	–
$K_{d(imm.\ SEC3\ or\ 3B2/sol.\ DR1)}$	μM	270[a]	4.6[a]
Independent Fits: Bimolecular Interactions			
$K_{d(3B2/TCR)}$	μM	–	18 ± 2
$K_{d(imm\ 3B2/sol.\ DR1)}$	μM	–	4.3 ± 1.4
$K_{d(sol.\ 3B2/sol.\ DR1)}$	μM	–	0.26 ± 0.07
Global Fits of Ternary Complex: Bimolecular Interactions			
$K_{d(3B2/TCR)}$	μM	–	22 ± 7
$K_{d(imm\ 3B2/sol.\ DR1)}$	μM	–	4.3 ± 1.4
$K_{d(sol.\ 3B2/sol.\ DR1)}$	μM	–	1.25 ± 1.0
Global Fits of Ternary Complex: Cooperative Interactions			
$\Delta G_{\alpha\beta}$	kcal/mol	–	-1.6 ± 0.3
$\Delta G_{V\beta}$	kcal/mol	–	0.8 ± 0.3
$\Delta G_{V\alpha}$	kcal/mol	–	-2.4 ± 0.1

[a] Data from ref *26*.

complex. Global fitting of combined data sets resulted in fits with root-mean-square deviation errors of approximately 10 RU, with all binding constants being well-determined. The results are presented in Table 1.

Representative examples from one such combined data set are shown in Figure 3. The upper panel clearly shows decreased binding of 3B2 to TCR β chain with increasing concentration of DR1. In the absence of any cooperativity, one would expect an increase in signal due to higher mass and therefore higher signal contribution of the 3B2−DR1 complex as compared to 3B2 alone (Figure 3A, dotted line). Since the amount of 3B2−DR1 complex in solution is known, as well as the binding constant of 3B2 to TCR β chain in the absence of DR1, this decrease in binding signal can be attributed to a reduced affinity of the 3B2−DR1 complex for the TCR β chain (i.e., negative cooperativity). Figure 3B shows the isotherm for ternary complex formation on the TCR $\alpha\beta$ heterodimer surface. In this representation, at any fixed DR1 concentration, increasing concentrations of 3B2 first exhibit an increase in ternary complex formation, followed by self-inhibition (i.e., decrease of ternary complex due to increased abundance of free 3B2). Cooperativity is indicated here by a higher affinity of the 3B2−DR1 complex for the TCR $\alpha\beta$ heterodimer than the affinity of 3B2 alone for the TCR $\alpha\beta$ heterodimer (Figure 3B, dotted lines). Inserted graphs in the lower panel show fits of the binary interactions. Note that the binding affinity of 3B2 for DR1 is approximately 10-fold higher in solution than when it is surface-bound (Table 1). While the reason for this is not clear, it cannot explain the observed cooperativity in our ternary protein complex as it affects complex formation in the presence or absence of the TCR α chain equally.

From modeling the two-dimensional isotherms, we estimate the overall free energy change due to cooperative binding ($\Delta G_{\alpha\beta}$) to be -1.6 ± 0.3 kcal/mol. By removing the TCR α chain, and thereby disrupting the cooperative basis for ternary complex formation, we measure a significant unfavorable cooperative free energy ($\Delta G_{V\beta}$) of 0.8 ± 0.3 kcal/mol, which indicates that simultaneous binding of TCR and DR1 to 3B2 has significant energetic costs. Finally, the energetic contribution of the DR1 β subunit−TCR α chain interactions ($\Delta G_{V\alpha} = \Delta G_{\alpha\beta} - \Delta G_{V\beta}$) was estimated to be -2.4 ± 0.1 kcal/mol. This translates into an approximately 50-fold increase in 3B2 affinity for TCR as a consequence of favorable cooperative interactions and illustrates the significance of the TCR Vα domain in maintaining the biological activity of SEC3. Moreover, higher stability of the ternary complex leads to lower minimal 3B2 concentrations at which ternary complex can be found, as well as higher 3B2 concentrations at which self-inhibition takes place. Thus, as a consequence of cooperative binding, the concentration range over which 3B2 cross-links TCR $\alpha\beta$ heterodimer and DR1 molecules is expanded.

Cooperative Binding Kinetics Are Temperature Dependent. For reactions possessing significantly unfavorable entropy, such as structural rearrangements of the combining site, dissociation and association rates become visibly slower at lower temperatures. Recent studies have shown that conformational flexibility is a general feature in the recognition of antigenic peptide−MHC complexes by TCR (*35*−*37*). To explore if molecular flexibility might be involved in the 3B2-mediated cross-linking of TCR $\alpha\beta$ heterodimer and DR1, the binding characteristics of various combinations of TCR $\alpha\beta$ heterodimer, 3B2, and DR1 were analyzed at temperatures ranging from 10 to 30 °C at 4 °C intervals (Figure 4). Binding of DR1 to immobilized 3B2 demonstrated temperature-dependent reaction kinetics, with binding kinetics slowing significantly as the temperature decreased (Figure 4A). The most likely mediators of temperature dependence in the 3B2−DR1 interaction are the N-terminal residues of the 3B2 disulfide loop, known to be highly flexible, which align to, and make contacts with, the α1 α helix of the DR1 molecule (E.J.S., P.S.A., and R.A.M., unpublished results). In contrast, the kinetics of 3B2 binding to TCR $\alpha\beta$ heterodimer were significantly less temperature dependent (Figure 4B). Combining 3B2 and DR1 in solution and monitoring for binding to immobilized TCR $\alpha\beta$ heterodimer (Figure 4C) showed a significant change in temperature effects relative to 3B2 binding in the absence of DR1, with the kinetics of this reaction being slower and more highly temperature dependent. The slower kinetics (at room temperature) of the ternary complex had previously been explained by cooperative binding (*26*). The increase in the temperature dependence of 3B2 binding to TCR $\alpha\beta$ heterodimer in the presence of DR1, however, can be explained equally well by flexibility contributed by the DR1 β subunit−TCR α chain interface in the ternary complex. Accordingly, no increase in temperature dependence on binding kinetics is seen in complexes lacking the TCR α chain (data not shown), indicating that 3B2 alone likely does not undergo substantial conformational change upon simultaneous binding to TCR and DR1. While this increase in the temperature dependence of binding kinetics in the 3B2-dependent cross-linking of TCR $\alpha\beta$ heterodimer and DR1 may not be linked to any specific biological function, it does demonstrate that cooperative binding may influence the molecular flexibility dynamics of some biomolecular interactions.

CONCLUSIONS

The sum of cooperative binding increases the overall TCR affinity of wild-type SEC3 to 1.4 μM, as calculated from the cooperative free energy of binding in this ternary complex, well within the affinity range described for native TCR ligands (*38*). Thus, we find that cooperative binding enhances the stability, and hence potency, of SEC3 to an

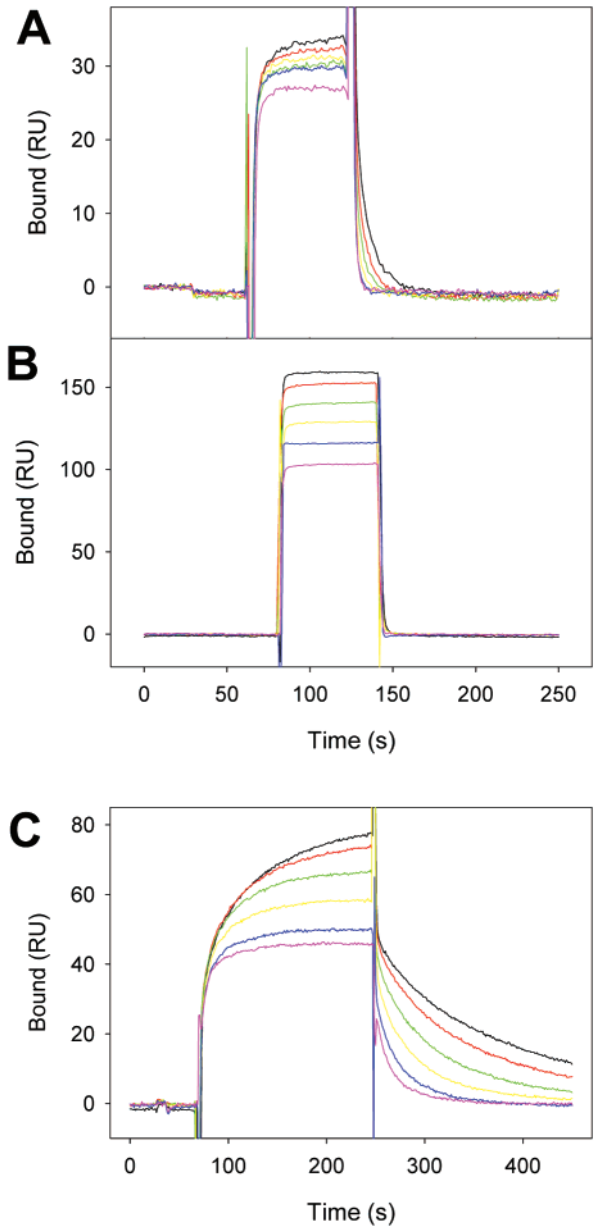

FIGURE 4: Effect of temperature on 3B2 binding. Overlay sensorgrams of binding reactions at selected equidistant temperatures ranging from 10 to 30 °C. (A) Binding of 8 μM DR1 to immobilized 3B2. (B) Binding of 20 μM 3B2 to immobilized TCR $\alpha\beta$ heterodimer. (C) Mixture of 4 μM 3B2 and 3 μM DR1 binding to immobilized TCR $\alpha\beta$ heterodimer. Colors of sensorgram traces are as follows: 10 °C, magenta; 14 °C, blue; 18 °C, yellow; 22 °C, green; 26 °C, red; 30 °C, black.

extent that each ternary complex adequately matches the TCR binding characteristics of agonist peptide−MHC ligands. The similarity in TCR binding strength of SEC3 and peptide−MHC ligands seems hardly coincidental and is likely the result of specific evolutionary pressures. Perhaps factors influencing the interface between T cells and antigen presenting cells, such as close alignment of opposing membranes (*39*) or formation of synapse-like structures (*40*, *41*), help stabilize the ternary complex to such an extent that maximum T cell activation is ensured even at relatively low intrinsic affinities. This, however, would not explain how cooperative binding can be beneficial to SEC3 function. It would seem simpler to evolve MHC−TCR cross-linkers that have two independent binding sites, each having a binding constant of about 1 μM, to mimic binding of the peptide−MHC ligands. Cross-linking with no cooperativity, however, as indicated in Figure 3B (dotted lines), narrows the range of concentrations at which SEC3 efficiently cross-links TCR and MHC molecules. Thus, cooperative binding expands the concentration range in which SEC3 efficiently stimulates T cells and hence increases toxin potency. The relatively modest magnitude of the energetic contribution to complex formation due to cooperativity could be due to limitations in the size of the MHC−TCR interface. Other cooperative systems involving similarly sized proteins binding to DNA (*13*−*17*) and cofactors (*18*, *19*), however, show free energy changes of magnitudes comparable to those reported here. While cooperative free energies are unlikely to be constrained to such a narrow range for all complexes involving multiple molecules, thermodynamic analysis of additional binding systems will be required to define their relevant physiological range.

In the present study, we provide an experimental and theoretical framework for investigating cooperative binding in a model ternary protein complex and show how this type of analysis can enhance our understanding of how the proteins involved function. As the methodology described is not particular to our cooperative binding system, it may be applicable to other molecular associations involving cooperativity. Alternative techniques for analyzing association energetics, such as isothermal titration calorimetry or fluorescence anisotropy, when merged with the mathematical modeling using standard laws of mass action and of mass balance, may also prove useful in dissecting cooperative systems. With the rates of discovery and structural description of multiprotein complexes involved in fundamental cellular processes increasing, the need for methods to quantitatively analyze cooperativity, a key energetic component of many of these reactions, is clear.

ACKNOWLEDGMENT

We thank D. H. Margulies for use of his BIAcore 2000 machine. The Basel Institute for Immunology was founded and is supported by Hoffmann-LaRoche Ltd., Basel, Switzerland.

REFERENCES

1. Uetz, P., Giot, L., Cagney, G., Mansfield, T. A., Judson, R. S., Knight, J. R., Lockshon, D., Narayan, V., Srinivasan, M., Pochart, P., Qureshi-Emili, A., Li, Y., Godwin, B., Conover, D., Kalbfleisch, T., Vijayadamodar, G., Yang, M., Johnston, M., Fields, S., and Rothberg, J. M. (2000) *Nature 403*, 623−627.
2. Walhout, A. J. M., Sordella, R., Lu, X., Hartley, J. L., Temple, G. F., Brasch, M. A., Thierry-Mieg, N., and Vidal, M. (2000) *Science 287*, 116−122.
3. McCraith, S., Holtzman, T., Moss, B, and Fields, S. (2000) *Proc. Natl. Acad. Sci. U.S.A. 97*, 4879−4784.
4. Rain, J.-C., Selig, L., De Reuse, H., Battaglia, V., Reverdy, C., Simon, S., Lenzen, G., Petel, F., Wojcik, J., Schachter, V., Chemama, Y., Labigne, A., and Legrain, P. (2001) *Nature 409*, 211−215.
5. Ito, T., Chiba, T., Ozawa, R., Yoshida, M., Hattori, M., and Sakaki, Y. (2001) *Proc. Natl. Acad. Sci. U.S.A. 98*, 4569−4574.
6. Bogan, A. A., and Thorn, K. S. (1998) *J. Mol. Biol. 280*, 1−9.
7. Lo Conte, L., Chothia, C., and Janin, J. (1999) *J. Mol. Biol. 285*, 2177−2198.

8. Sundberg, E. J., and Mariuzza, R. A. (2000) *Structure 8*, 137−142.
9. Ma, B., Wolfson, H. J., and Nussinov, R. (2001) *Curr. Opin. Struct. Biol. 11*, 364−369.
10. Sundberg, E. J., and Mariuzza, R. A. (2002) *Adv. Protein Chem.* (in press).
11. Courey, A. J. (2001) *Curr. Biol. 11*, R250−R252.
12. Germain, R. N., and Stefanova, I. (1999) *Annu. Rev. Immunol. 17*, 467−522.
13. Darling, P. J., Holt, J. M., and Ackers, G. K. (2000) *J. Mol. Biol. 302*, 625−638.
14. Abbott, J., and Beckett, D. (1993) *Biochemistry 32*, 9649−9656.
15. Burz, D. S., and Ackers, G. K. (1994) *Biochemistry 33*, 8406−8416.
16. Librizzi, M. D., Moir, R. D., Brenowitz, M., and Willis, I. M. (1996) *J. Biol. Chem. 271*, 32695−32701.
17. Wilson, G. M., Sutphen, K., Bolikal, S., Chuang, K., and Brewer, G (2001) *J. Biol. Chem. 276*, 44450−44456.
18. Bradick, T. D., Beechem, J. M., and Howell, E. E. (1996) *Biochemistry 35*, 11414−11424.
19. Roitel, O., Sergienko, E., and Branlant, G. (1999) *Biochemistry 38*, 16084−16091.
20. Wells, J. A., and de Vos, A. M. (1996) *Annu. Rev. Biochem. 65*, 609−634.
21. Kerpolla, T. K. (1998) *Structure 6*, 549−554.
22. Koudelka, G. B. (2000) *Curr. Biol. 10*, R704−R707.
23. Wallny, H. J., Sollami, G., and Karjalainen, K. (1995) *Eur. J. Immunol. 25*, 1262−1266.
24. Bentley, G. A., Boulot, G., Karjalainen, K., and Mariuzza, R. A. (1995) *Science 267*, 1984−1987.
25. Frayser, M., Sato, A. K., Xu, L., and Stern, L. J. (1999) *Protein Expression Purif. 15*, 105−114.
26. Andersen, P. S., Lavoie, P. M., Sekaly, R. P., Churchill, H., Kranz, D. M., Schlievert, P. M., Karjalainen, K., and Mariuzza, R. A. (1999) *Immunity 10*, 473−483.
27. Leder, L., Llera, A., Lavoie, P. M., Lebedeva, M. I., Li, H., Sekaly, R. P., Bohach, G. A., Gahr, P. J., Schlievert, P. M., Karjalainen, K., and Mariuzza, R. A. (1998) *J. Exp. Med. 187*, 823−833.
28. Li, H., Llera, A., Malchiodi, E. L., and Mariuzza, R. A. (1999) *Annu. Rev. Immunol. 17*, 435−466.
29. Garcia, K. C., Degano, M., Stanfield, R. L., Brunmark, A., Jackson, M. R., Peterson, P. A., Teyton, L., and Wilson, I. A. (1996) *Science 274*, 209−219.
30. Fields, B. A., Malchiodi, E. L., Li, H., Ysern, X., Stauffacher, C. V., Schlievert, P. M., Karjalainen, K., and Mariuzza, R. A. (1996) *Nature 384*, 188−192.
31. Brünger, A. T., Adams, P. D., Clore, G. M., DeLano, W. L., Gros, P., Grosse-Kunstleve, R. W., Jiang, J. S., Kuszewski, J., Nilges, M., Pannu, N. S., Read, R. J., Rice, L. M., Simonson, T., Warren, G. L. (1998) *Acta Crystallogr., Sect. D: Biol. Crystallogr. 54*, 905−921.
32. Gascoigne, N. R., and Ames, K. T. (1991) *Proc. Natl. Acad. Sci. U.S.A. 88*, 613−616.
33. Malchiodi, E. L., Eisenstein, E., Fields, B. A., Ohlendorf, D. H., Schlievert, P. M., Karjalainen, K., and Mariuzza, R. A. (1995) *J. Exp. Med. 182*, 1833−1845.
34. Andersen, P. S., Geisler, C., Buus, S., Mariuzza, R. A., and Karjalainen, K. (2001) *J. Biol. Chem. 276*, 33452−33457.
35. Garcia, K. C., Degano, M., Pease, L. R., Huang, M., Peterson, P. A., Teyton, L., and Wilson, I. A. (1998) *Science 279*, 1166−1172.
36. Boniface, J. J., Reich, Z., Lyons, D. S., and Davis, M. M. (1999) *Proc. Natl. Acad. Sci. U.S.A. 96*, 11446−11451.
37. Willcox, B. E., Gao, G. F., Wyer, J. R., Ladbury, J. E., Bell, J. I., Jakobsen, B. K., and van der Merwe, P. A. (1999) *Immunity 10*, 357−365.
38. Davis, M. M., Boniface, J. J., Reich, Z., Lyons, D., Hampl, J., Arden, B., and Chien, Y. (1998) *Annu. Rev. Immunol. 16*, 523−544.
39. Dustin, M. L., Golan, D. E., Zhu, D. M., Miller, J. M., Meier, W., Davies, E. A., and van der Merwe, P. A. (1997) *J. Biol. Chem. 272*, 30889−30898.
40. Monks, C. R., Freiberg, B. A., Kupfer, H., Sciaky, N., and Kupfer, A. (1998) *Nature 395*, 82−86.
41. Grakoui, A., Bromley, S. K., Sumen, C., Davis, M. M., Shaw, A. S., Allen, P. M., and Dustin, M. L. (1999) *Science 285*, 221−227.

BI0200209